Supporting Information for "Photo-induced and Thermal Bistability of Spin Crossover Nano-particles"

Nadeem Natt and Benjamin J. Powell*

School of Mathematics and Physics, The University of Queensland, Brisbane, Queensland, 4072, Australia

E-mail: powell@physics.uq.edu.au

Supporting Information Available

Model and Method

We employ a recently developed semi-classical, semi-empirical SCO model[1–3] to investigate T_{LIESST} and $T_{1/2}$ in nanoparticles based on d^6 metals. The model combines single molecular SCO dynamics with elastic inter-molecular interactions. One symmetric breathing coordinate (Q_i) of each SCO complex is explicitly considered via potential energy surfaces calculated from crystal field theory. For a single molecule, the model consists of four adiabatic free energy surfaces, figure S1. The most important of these states is a non-degenerate double-well state that mixes LS, HS and intermediate spin states via the spin-orbit interaction. The double well state introduces kinetic barriers between the LS and HS states. In addition to the double well, there are three pure HS adiabatic free energy surfaces, each with different multiplicities, figure S1. The spin state and magnetic susceptibility of the single molecular model smoothly depend on Q_i.[1]

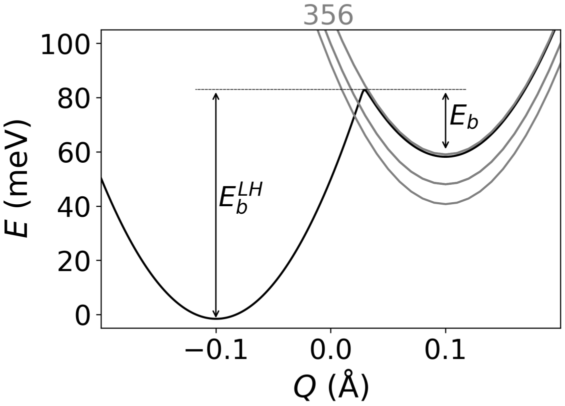

Figure S1: Schematic representation of the theoretical model for SCO nanoparticles, equation 1. Intramolecular free energy surfaces along fully symmetric coordinate (Q) at 0 K for the default set of parameters given in table S1. E_b and E_b^{LH} are the single molecular kinetic barriers in non-degenerate double well state for HS→LS and LS→HS, respectively. The pure HS states are plotted as grey lines and the their degeneracies labelled.

The adiabatic free energy surfaces of d^6 complexes depend on the ligand-field strength, Dq, the Racah parameters, B and C, spin-orbit coupling strength, ζ, the symmetric mode force constant, k, the metal-ligand bond length difference between the HS and LS states, 2δ, the average of the molecular frequencies in the HS, ω_{HS}, and LS, ω_{ls}, states, and the temperature, T. Typical parameters for the SCO complexes have been estimated from the experimental literature on Fe(II) complexes[1] and are reproduced in table S1.

To model the bare SCO-NPs, we place spin-crossover centres on a square or cubic lattice with classical elastic interactions between neighbours, as sketched in figure 1b. Intermolecular elastic interactions are modelled as springs between pairs of neighbours, with force constants $k_n > 0$ between nth nearest neighbours, where $n = 1, 2$, or 3. The model Hamiltonian is

$$H = \sum_i^N \left[\frac{\mathbf{p}_i^2}{2m} + \frac{\mathbf{P}_i^2}{2M} + V_{\nu,i}^{\text{SCO}}(Q_i) + \sum_{<i,j>_n} U_n(Q_i, Q_j, \mathbf{r}_i, \mathbf{r}_j) \right], \tag{S1}$$

where $V_{\nu,i}^{\text{SCO}}(Q_i)$ is the vth adiabatic potential energy surface of the ith spin-crossover molecule; $\mathbf{r}_i$ is position of the ith molecule with mass m and conjugate momentum $\mathbf{p}_i$; M is the mass associated with the momentum, $\mathbf{P}_i$, of the breathing coordinate, Q_i; and U_n is the potential energy between two neighbouring sites. The elastic interaction between a pair is

$$U_n(Q_i, Q_j, \mathbf{r}_i, \mathbf{r}_j) = \frac{k_n}{2}\Big(|\mathbf{r}_i - \mathbf{r}_j| - \mu_n(a_c + Q_i + Q_j)\Big)^2, \tag{S2}$$

where $\mu_1 = 1$, $\mu_2 = \sqrt{2}$, $\mu_3 = \sqrt{3}$ and a_c is the average of the $T = 0$ lattice constants of the all-LS and all-HS states.

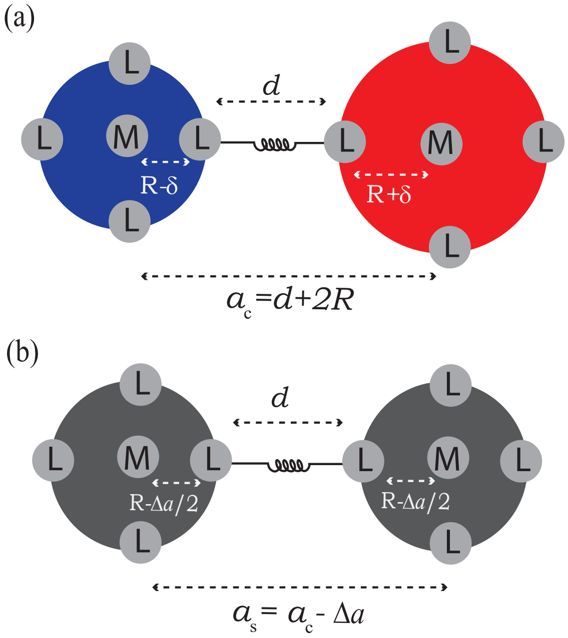

Figure S2: Pictorial representation of the core-shell lattice mismatch (Δa). 0 K equilibrium distances between (a) nearest neighbour LS and HS SCO sites and (b) a pair of nearest neighbour shell sites are $a_c = d + 2R$ and $a_s = a_c + \Delta a$ respectively. M and L represent metals and ligands, δ is the metal-ligand bond length difference between the HS and LS states, and R and d are constants.

The instantaneous size of a spin-crossover metal-ligand coordination sphere is $Q_i + R$, where R is the average of 0 K equilibrium bond lengths of the HS and LS states, figure S2. The double well intramolecular potential energy surface of spin crossover, figure S1, has minima at $Q_i = \delta$ for the HS state and $Q_i = -\delta$ for the LS state. Thus, the 0 K equilibrium bond length of the LS state is $R - \delta$ and that of the HS state is $R + \delta$. We denote the

0 K equilibrium distance between the nearest ligands of nearest neighbours d, figure S2. Therefore, the core lattice constant (0 K equilibrium distance between nearest neighbour spin crossover HS and LS sites) is $a_c = d + 2R$, figure S2.

We wish to consider non-SCO shells, such as silica or non-SCO transition metal complexes and framework materials. The natural physical picture for these different shells is quite different. However, because of the well known properties of networks of springs, all reasonable physical models of networks of springs should be mathematically equivalent once the choice of parameters has been modified appropriately. The simplest picture to implement in our computational framework is that of non-SCO transition metal complexes, sketched in figure 1c, so we adopt that here.

For simplicity, we assume that the intra-complex ligand-ligand bond length, d, and the intramolecular interactions, Eq S2, are the same in the non-SCO shell, the SCO core and interface between the shell and the core. This means that any difference in lattice constant between the core and the shell arises from the inner coordination sphere, figure S2. Thus if the the 0 K shell lattice constant, is $a_s = a_c - \Delta a$, S2, then the equilibrium value of Q_i for non-SCO shell sites is $-\Delta a/2$. Thus, shell sites are described by a single intramolecular potential energy surface,

$$V^{\text{shell}}(Q_i) = \frac{k}{2}\left(Q_i + \frac{\Delta a}{2}\right)^2. \tag{S3}$$

We model $N \times N$ two-dimensional and $N \times N \times N$ three-dimensional NPs on square and cubic lattices respectively, where N is the total edge length. The finite systems are modelled using the classical molecular dynamics methods[1] at constant temperature using the Nose-Hoover thermostat.[4] To model the finite-size effect of NPs, we employ open boundary conditions. To model the infinite bulk systems periodic boundary conditions are applied with Anderson barostat[4] at zero pressure.[1,2] For SCO sites, the occupation of the intramolecular free energy surfaces V_ν^{SCO} was determined via 20 metropolis Monte-Carlo steps after every 50 molecular dynamics steps, at fixed positions and forces.

To calculate the thermal SCO behaviour of a SCO-NP, we initialise the NP at a high temperature (e.g. 250 K) in the all-HS state and cool down to 10 K before warming to the all-HS state again. For the thermally-activated relaxation of the trapped excited state, we initialise the sample at the all-HS state at 10 K and slowly warm the trapped HS state. We calculate ensemble average of magnetic susceptibility (χ) at each temperature and obtain $T_{1/2}$, $\Delta T_{1/2}$ and T_{LIESST} from χT. Half of the population switches spin state on heating from low T at $T_{1/2\uparrow}$, whereas at $T_{1/2\downarrow}$ half of the population switches spin state on cooling from high T. T_{LIESST} is the minimum in $\partial(\chi T)/\partial T$, obtained from warming the initialized all-HS state at 10 K.

Table S1: Values of the parameters used in all of the calculations presented in this paper. The values are within the typical range estimated for Fe(II) materials and previously discussed in reference.[1] Different elastic parameters were selected for two and three dimensions to give transitions with simliar $T_{1/2}$, $\Delta T_{1/2}$, and T_{LIESST} for bare SCO-NPs in both cases. Here B and C are Racah parameters, $10Dq$ is the ligand field splitting, ζ is the spin-orbit interaction strength, k is the spring constant of the metal ligand bonds in the IS state, δ is the decrease (increase) in the metal-ligand bond length in the LS (resp. HS) state relative to the IS state, ω_{LS} (ω_{HS}) is the average frequency of the implicit modes in the LS (resp. HS) state, k_n is the spring constant between nth nearest neighbours ($n = 1, 2$, or 3), and a_{c} is the lattice constant of the core.

Parameter	**Value**	
	2D	3D
B	100 meV	
C/B	4.81	
Dq/B	2.0324	
ζ	14.66 meV	
k	10.34 eV/Å^2	
δ	0.1 Å	
ω_{HS}	5×10^{13} s^{-1}	
ω_{LS}	8×10^{13} s^{-1}	
k_1	0.86 eV/Å^2	0.689 eV/Å^2
k_2	$0.2k_1$	$0.625k_1$
k_3	0	$0.375k_1$
a_{c}	9.80 Å	

Simplified model of the barrier height, E_b

In this section, we study a toy version of our model, that can be solved exactly. This allows us to calculate the height of the barrier between the HS and LS states and thus its dependence on the relative energies of the HS and LS states, ΔH.

To this end we consider a single molecule with a diabatic LS state that has energy

$$E_L = \frac{k}{2}\left(Q+\delta\right)^2 \tag{S4}$$

and a single diabatic HS state with energy

$$E_H = \frac{k}{2}\left(Q-\delta\right)^2 + \Delta H \tag{S5}$$

where Q is the coordinate describing the breathing mode of the molecule.

If these two modes are coupled by a second-order spin-orbit coupling matrix element,[1] λ, the barrier height on the lowest adiabatic state is straightforwardly calculated to be

$$E_b = \frac{(2k\delta^2 - \Delta H)^2}{8k\delta^2} - \lambda \simeq \frac{(2k\delta^2 - \Delta H)^2}{8k\delta^2}. \tag{S6}$$

In the final approximation, we have assumed that λ is small compared to the energy difference between the crossing off the two parabolas and the minimum of the HS level. From the full model, we find[1] that $\lambda = 1.32$ meV for the default parameter values of table S1, in good agreement with this approximation.

Finally, we plot the variation of E_b with ΔH in figure 4d, with all other parameters set to the values given in table S1. This shows that, in the physically relevant parameter range, E_b decreases as ΔH increases.

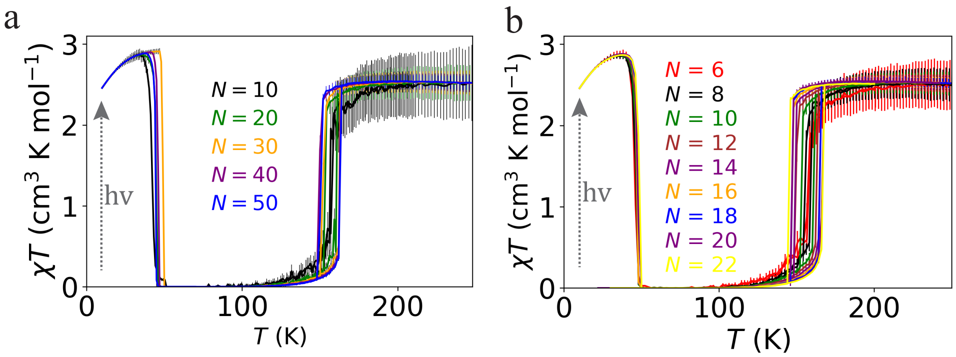

Figure S3: Calculated magnetic susceptibility of bare SCO-NPs for thermal SCO and thermally activated relaxation of trapped HS state, as discussed in figure 2. (a) For 2D NPs. Here, $k_1 = 0.86$ eV/Å^2 and $k_2 = 0.2k_1$ the rest of the parameters are given in table 1. (b) For 3D NPs. Here $k_1 = 0.689$ eV/Å^2, $k_2 = 0.625k_1$ and $k_3 = 0.375k_1$ and the rest of the parameter values are given in table S1.

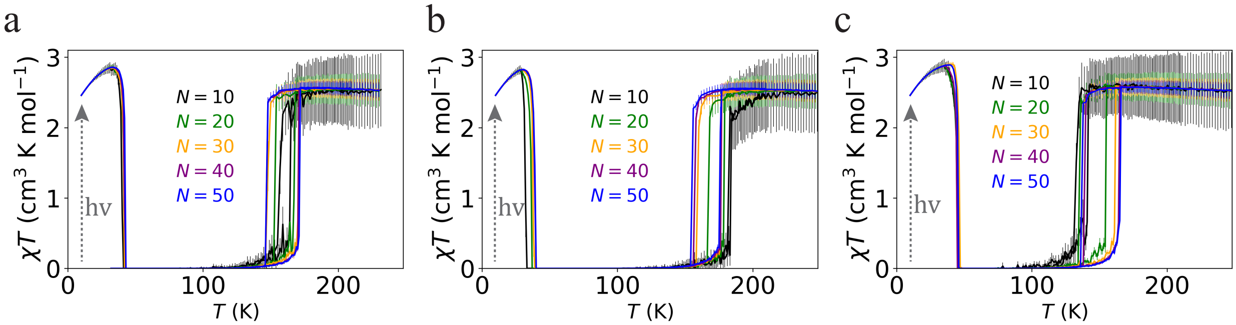

Figure S4: Calculated magnetic susceptibility of core-shell 2D core-shell SCO-NPs for thermal SCO and thermally activated relaxation of trapped HS state, as discussed in figure 3b-d. Here we study NP size changes at a fixed shell thickness $N_s = 1$ and core-shell lattice mismatch (a) $\Delta a = 0$, (b) $\Delta a = 0.2\mathring{A}$, and (c) $\Delta a = -0.2\mathring{A}$.

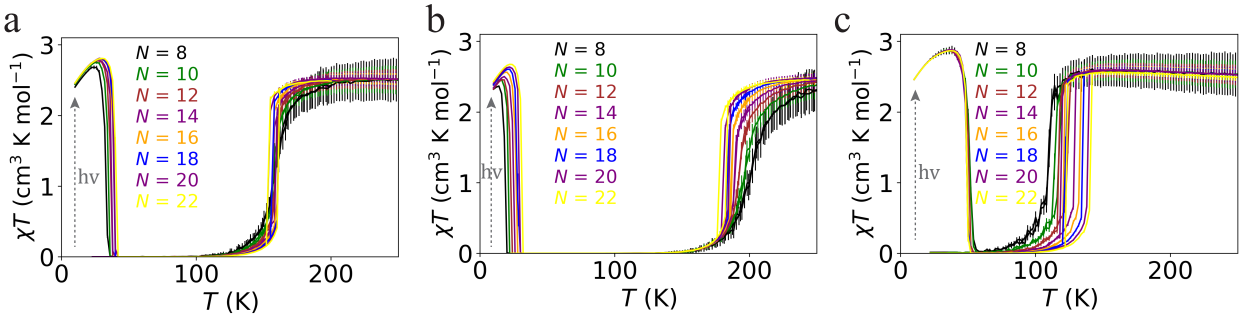

Figure S5: Calculated magnetic susceptibility of 3D core-shell SCO-NPs for thermal SCO and thermally activated relaxation of trapped HS state, as discussed in figure 3d-h. Here we study NP size changes at a fixed shell thickness $N_s = 1$ and fixed core-shell lattice mismatch (a) $\Delta a = 0$, (b) $\Delta a = 0.2\mathring{A}$, and (c) $\Delta a = -0.2\mathring{A}$. Here $k_1 = 0.689$ eV/Å^2, $k_2 = 0.625k_1$ and $k_3 = 0.375k_1$ and the rest of the parameter values are given in table S1.

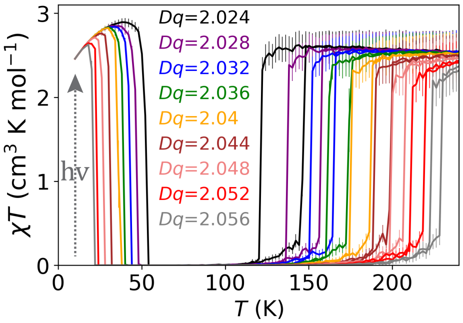

Figure S6: Calculated magnetic susceptibility of 2D core-shell SCO-NPs for thermal SCO and thermally activated relaxation of trapped HS state, as discussed in figure 4c. Here we study the effect of ligand field strength at a fixed shell thickness $N_s = 1$, NP size $N = 20$, and $\Delta a = 0$. Here, $k_1 = 0.86$ eV/Å^2 and $k_2 = 0.2k_1$ and the rest of the parameter values are given in table S1.

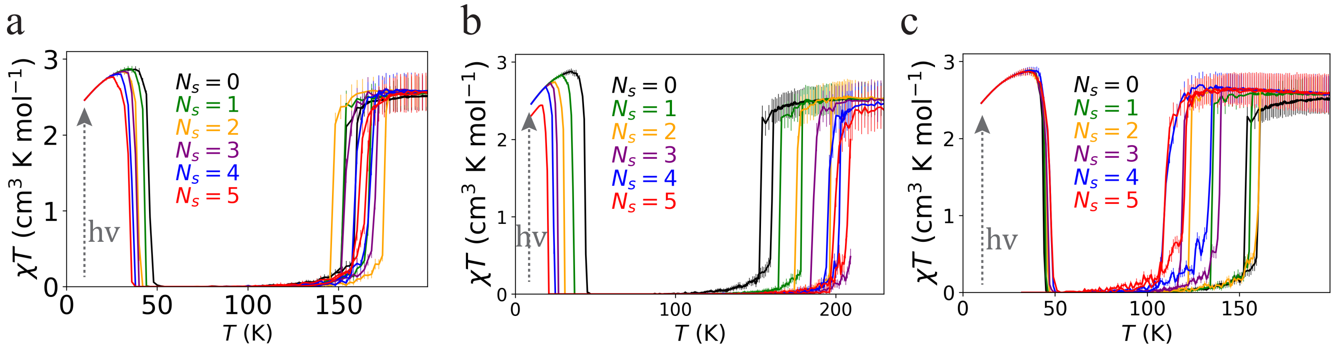

Figure S7: Calculated magnetic susceptibility of 2D core-shell SCO-NPs for thermal SCO and thermally activated relaxation of trapped HS state, as discussed in figure 5a,b. Here we study the effect of shell thickness N_s at a fixed core size $N_c = 20$, and core-shell lattice mismatch (a) $\Delta a = 0$, (b) $\Delta a = 0.2\mathring{A}$, and (c) $\Delta a = -0.2\mathring{A}$. Here, $k_1 = 0.86$ eV/Å^2 and $k_2 = 0.2k_1$ and the rest of the parameter values are given in table S1.

References

(1) Nadeem, M.; Cruddas, J.; Ruzzi, G.; Powell, B. J. Toward high-temperature light-induced spin-state trapping in spin-crossover materials: the interplay of collective and molecular effects. *J. Am. Chem. Soc.* **2022**, *144*, 9138–9148.

(2) Natt, N.; Powell, B. J. Complex relaxation of trapped spin-states in spin crossover materials. *Chemical Science* **2024**, *15*, 17862–17872.

(3) Yuan, S.; Natt, N.; Powell, B. J. Impact of Molecular Distortions on Bistability in Spin Crossover Complexes. *Inorganic Chemistry* **2025**, *64*, 7182–7193.

(4) Nosé, S. A unified formulation of the constant temperature molecular dynamics methods. *J. Chem. Phys.* **1984**, *81*, 511–519.